Journal of Catalysis **184,** 29–38 (1999)
Article ID jcat.1999.2431, available online at http://www.idealibrary.com on IDEAL®

EPR and NMR Studies of Coke Induced Selectivation over H–ZSM-5 Zeolite during Ethylbenzene Disproportionation Reaction

Ajit R. Pradhan,*[,1] Tien-Sung Lin,† Wen-Hua Chen,* Sung-Jeng Jong,*[,2]
Jin-Fu Wu,* Kuei-Jung Chao,‡ and Shang-Bin Liu*[,3]

*Institute of Atomic and Molecular Sciences, Academia Sinica, P.O. Box 23-166, Taipei, Taiwan 106, Republic of China; †Department of Chemistry, Washington University, St. Louis, Missouri 63130; and ‡Department of Chemistry, National Tsinghua University, Hsinchu, Taiwan 300, Republic of China

Received April 21, 1998; revised January 13, 1999; accepted January 19, 1999

A combination of EPR, ^{13}C CP-MAS NMR, ^{129}Xe NMR, xenon adsorption, and TGA techniques were employed to examine the preferred location of coke formation in the conversion of ethylbenzene (EB) under various conditions, such as reaction temperature, space velocity, and carrier gas (H_2) to EB molar ratio. Effects of coking conditions on the nature of coke as well as on the selectivity of *p*-diethylbenzene were studied in parallel so that the correlation between the coke structure and product shape selectivity can be inferred. An increase in reaction temperature resulted in the formation of coke residues consisting of condensed polycyclic aromatic compounds. On the other hand, a change in space velocity and H_2/EB molar ratio did not lead to any notable change in the composition of the coke. However, increases in the reaction temperature and space velocity or decreases in the H_2/EB ratio tend to enhance *para*-selectivity using the H–ZSM-5 zeolite. The induced shape selectivity is ascribed to the preferential deposition of the coke on the external surfaces of the H–ZSM-5 crystallites. Thus, the use of coke as a modifying agent for selectivation of a H–ZSM-5 zeolite in an EB disproportionation reaction is demonstrated.

Key Words: **coking; H–ZSM-5 zeolite; selectivity; NMR; EPR; ethylbenzene disproportionation.**

INTRODUCTION

During disproportionation of monoalkylbenzenes over ZSM-5 zeolite, an equilibrium mixture of di-alkylbenzene isomers is always attained even at low conversion. This is attributed to the rate of isomerization of di-alkylbenzene isomers being always greater than the rate of disproportionation of monoalkylbenzenes (1). For example, the rate of isomerization is 7000 times higher than the rate of disproportionation in the toluene disproportionation reaction. Thus, the primary product *p*-xylene formed under the steric constraints imposed by the medium pore zeolite ZSM-5 is further isomerized into *m*- and *o*-xylene, and an equilibrium mixture of isomers is obtained as the final products. Previously, Chen *et al.* (2) reported a specific technique to determine the conditions for enhancing the *p*-selectivity in the toluene disproportionation reaction. They showed that the *p*-selectivity enhancement could be achieved if the rate of isomerization was reduced by mass transport constraints.

In principle, one may increase the *p*-isomer selectivity by the retardation of the bulkier *m*- and *o*-isomers imposed by the diffusion constraints, i.e., applying zeolite catalyst with greater crystalline size. As a result, the purpose of enhancing *p*-isomer yield is served. More recently, Niwa *et al.* (3) reported that the product shape selectivity in applying zeolite ZSM-5 strongly depends on the size of crystals, an important adsorption property of zeolites. They also indicated that the acidity on the external surfaces was not a prevailing factor to control the shape selectivity of zeolites. However, it is difficult to prepare very large ZSM-5 crystals in large quantity; therefore the attainment of high *p*-selectivity by this option is limited (4).

Chen *et al.* (5) were the first to demonstrate that high selectivity in alkylation or disproportionation of monoalkylbenzenes can be obtained by means of chemical modification of the crystalline surface of zeolite catalyst. Such modification can be achieved by depositing bulky phosphorous or magnesium compounds, or large organic molecules on the surface. Note that these compounds are too big to enter the zeolite pores or channels. In other words, the modification is to block the active sites on the external surface and/or to decrease the pore–channel apertures of the zeolite. For instance, surface chemical vapor deposition (CVD) utilizing silicon alkoxide (6) has been employed to enhance shape selectivity of zeolites. The deposited silica serves not only to reduce the free diameter of the pore–channel apertures, but also to deactivate the external surface of zeolites. This method has been applied in various types of zeolites with marked improvements in catalytic functions,

[1] Present address: Department of Chemistry, Purdue University, West Lafayette, IN 47907.

[2] Present address: Union Chemical Laboratory, Industrial Technology Research Institute, Hsingchu, Taiwan 300, R.O.C.

[3] To whom correspondence should be addressed.

0021-9517/99 $30.00

such as product selectivity in disproportionation, cracking and alkylation of alkylbenzenes, and in aromatization reactions (7–12).

A more convenient and economical way to enhance shape selectivity in zeolite catalysts is by selective coke deposition. Haag and Olson (13) reported a unique coke selectivation method that effectively modified their catalyst to achieve an 80–90 wt% yield of *p*-xylene. The high shape selectivity of the modified catalyst was attributed to the blocking of the external active site and the narrowing of the pore mouth by coking. Uguina *et al.* (14) showed that the amount, the nature, and the location of the carbonaceous residues in the formation of coke could affect the shape selectivity, which in turn depends strongly on the nature of the hydrocarbon reactants which may further react to form coke precursors. For instance, they reported that coking with isobutene gave rise to the formation of intracrystalline coke, which yielded a notable decrease in toluene conversion while the *p*-selectivity was maintained. On the other hand, cokes formed from mesitylene tend to deposit on the external surface of zeolites and resulted in an increase in *p*-selectivity during toluene conversion. For those formed from toluene, cokes tend to deposit both on the external surfaces and within the internal zeolite voids. Such a deposition producing high *p*-selectivity in toluene conversion is similar to what was observed in the uncoked ZSM-5 zeolite.

On the other hand, Èejka *et al.* (15) reported a negative effect; the *p*-selectivity in toluene alkylation reaction decreased with increasing coke concentration utilizing H–ZSM-5. Rozwadowski *et al.* (16) also reported that the ratio of external to internal coke deposition increased with the reaction temperature during methanol conversion. Moreover, the ratio of polycyclic aromatics to aliphatic compounds of the coke deposits was also observed to increase with reaction temperature. In a catalytic study of ZSM-5 zeolite during alkylation of ethylbenzene (EB) with ethanol, Bhat *et al.* (17) reported that when the external surfaces of the zeolite catalyst were modified by the combination of silicon CVD and coking, an increase in the stabilization of catalytic activity was observed. Recently, Melson and Schüth (18) showed that using a set of samples with the same Si/Al ratio but varied particle sizes in EB disproportionation utilizing H–ZSM-5 zeolite, the conversion and product distribution were strongly dependent on the external acidity, which in turn was correlated well with the particle size. Fang *et al.* (19) further demonstrated that the conversion and coke induced *p*-xylene selectivity could be fine tuned by carefully controlled reaction conditions, such as temperature, duration of the reaction, and type and concentration of the carrier gases during toluene disproportionation over H–ZSM-5 zeolite.

Catalysts with high shape selectivity are always in urgent demand in the petrochemical and the fine chemical industrial processes. However, systematic efforts made on the investigation and evaluation of the coke selectivation process are conspicuously lacking. The objectives of the present study are two-fold: (1) to evaluate the use of coke as a modifying agent of zeolite during an EB disproportionation reaction and (2) to examine the shape selectivity of products induced by modified coke under specific controllable experimental conditions. We employed a combination of EPR, NMR, adsorption, GC, and TGA techniques to study the effects of coking conditions such as reaction temperature (T_c), space velocity (WHSV), and carrier gas to feed ratio (i.e., H_2/EB molar ratio) on the nature and location of coke. The variations in product shape selectivity induced by coking were monitored by ^{129}Xe NMR and by the distribution of product analyses in the transformation of EB.

EXPERIMENTAL

Materials and Sample Preparation

The acid form of ZSM-5 zeolite (Si/Al = 15) was obtained from PQ zeolite B.V. Powder X-ray diffraction and ^{29}Si magic-angle-spinning (MAS) NMR confirmed the structure and framework compositions of the sample. The average particle size of the powdered, binderless sample is ca. 0.3 μm as established by electron microscopy. The amount of NH_3 retained in the sample at 200°C was 0.79 millimoles per gram of catalyst. Complementary experiments were carried out with another H–ZSM-5 sample (Si/Al = 33) having larger crystalline size (ca. 2 μm) and spherical morphology. Detailed experimental procedures and characterization of the sample are reported elsewhere (20). Ethylbenzene (A.R. grade), obtained from Merck-Schuchardt, was used without further purification.

Prior to the selective coking, pelletized zeolite catalyst (10–20 mesh, ca. 4 g) was activated at 500°C in air for 8 h. It was brought to reaction conditions first in the presence of nitrogen and then hydrogen. Coking was carried out in a continuous flow reactor system using EB as the precursor. The coking conditions were as follows: reaction temperature (T_c: 350–550°C), carrier gas to reactant feed molar ratio (H_2/EB: 0-1), and space velocity (WHSV: 13–50 h^{-1}) in their respective range. The reaction was allowed to be carried out for 3 h of time-on-stream (TOS), then the catalyst was purged with H_2 for 1 h under the same experimental conditions before it was brought to room temperature (25°C). The liquid products were analyzed by gas chromatography (Shimadzu GC-9A) with a 5% SP-1200 and 1.75% Bentone 34 on 100/120 Suplecoport packed column. To study the effects of coke induced shape-selectivity, some of the experiments were repeated to test the activity. Here, the reactions were brought to the standard reaction conditions, namely $T_c = 260$°C, H_2/EB = 2, WHSV = 3.5 h^{-1}, and TOS = 2 h, after selective coking.

Characterization Methods

The amount of coke formed during selective coking was measured by thermogravimetric analysis on a thermogravimeter (ULVAC TGD 7000RH) using air as a carrier gas at a heating rate 10°C min^{-1}. The weight-loss between 300 and 700°C was reported as the total coke content. Prior to the study, all fouled samples were stored over saturated NaCl solution in a desiccator for at least 24 h.

Before the EPR or the ^{129}Xe NMR experiments, all the coked samples were dehydrated by gradual heating to 200°C under vacuum ($<10^{-5}$ Torr, 1 Torr = 133.32 Pa). The samples were maintained at that temperature for at least 18 h. The configuration of the sample tube was designed so that a standard quartz (or NMR) tube joined to a vacuum stopcock could be conveniently used in thermal treatment or adsorption of xenon molecules on a vacuum apparatus. An X-band EPR spectrometer (Bruker ER 300) was employed for EPR measurements at room temperature. A sample of diphenyl picryl hydrazyl (DPPH; $g = 2.0037$) was used as the g-value marker. Spin concentration was measured by double integration of the EPR signal and compared with the known spin count of DPPH.

^{129}Xe NMR experiments were performed on a Bruker MSL-300P NMR spectrometer operating at 83.012 MHz. The ^{129}Xe NMR chemical shifts were referred to that of Xe gas at extreme dilution. Xenon adsorption isotherms were measured at room temperature by the volumetric method. ^{13}C CP-MAS NMR experiments were performed on a Bruker MSL-500P spectrometer at a resonance frequency of 125.77 MHz. All spectra were obtained with proton decoupling. A contact time of 2 ms was used in the cross-polarization experiments. Typically, 30,000–90,000 free induction decay (FID) signals were accumulated using a recycle delay of 1 s. The ^{13}C NMR chemical shift was measured relative to tetramethylsilane (TMS). All FIDs were subjected to exponential multiplication to enhance the spectral sensitivity. As a result, an artificial linewidth of 100 Hz was introduced during spectral processing. Detailed experimental setup and experimental procedures were reported previously (21, 22).

RESULTS

Product Analysis

The product analysis showed that the conversion of EB was more than 80 wt% (TOS = 3 h) under all experimental conditions (*vide ante*). Among the liquid products, benzene was the major product (40–60 wt%) which formed during the dealkylation reaction. Other minor products were toluene (5–10 wt%), xylenes (2–4 wt%), C_9–C_{11} aromatics (1–2 wt%), diethylbenzenes (1–5 wt%), and C_{12+} aromatics (4–6 wt%). Among the gaseous products formed during the transformation, ethylene was identified as the major product. The relative composition of the products varied with the reaction conditions and the degree of coking.

Thermogravimetric Analysis

The thermograms of the deactivated samples obtained during selective coking under various reaction conditions were individually recorded. The amount of total coke retained in the spent sample was determined by the relative weight loss during the temperature range 300–700°C, as presented in Table 1. The overall coke content varied from 3.3 to 4.5 wt% depending on the reaction conditions. In general, the amount of total coke increased with increasing reaction temperature in the range $350°C \le T_c \le 550°C$. The same trend was found for the concentration variation of carrier gas in the range $0 \le H_2/EB \le 1$ whereas no apparent trend was found in varying the space velocity.

EPR Studies

EPR spectroscopy was employed to characterize the coke formed on the zeolite catalyst. The EPR spectra of the coked samples obtained under various reaction conditions are presented in Fig. 1. The observed changes in the spectral parameters as a function of reaction temperature (at constant $H_2/EB = 0.5$ and WHSV = 13 h^{-1}) are summarized in Table 1. The spectral linewidth and the g value were both observed to decrease with increasing T_c, while the spin concentration (per gram of coke, denoted χ) increased from 2.4×10^{18} at 350°C to 1.3×10^{20} at 550°C, a 54-fold increase. No hyperfine splitting of the multiple line was observed in the reaction temperature range of our studies. This is in contrast to the previously reported EPR studies of coke formed during ethylene reaction over H–mordenite (23, 24) where multiple EPR lines in the temperature range 107–137°C were reported. Note that the H–mordenite studies were performed in the low temperature (soft) coke domain. The authors attributed the multiple EPR lines to the formation of olefinic or allylic carbonaceous compounds. However, our spectral analyses showed that the carbonaceous compounds were mostly polycyclic aromatic compounds in nature.

In the coke characterization as a function of the H_2/EB molar ratio at fixed $T_c = 500°C$ and WHSV = 13 h^{-1}, we observed that the spectral linewidth increased marginally with increasing H_2/EB ratio (Table 1). This spin concentration showed little variation with respect to different H_2/EB ratios, decreasing from 1.7×10^{20} to 1.3×10^{20} when the H_2/EB ratio increased from near zero to one. The g-value of EPR signals remained the same.

In the spectral velocity dependent studies, at constant $T_c = 500°C$ and $H_2/EB = 0.5$, we observed that the spectral linewidth increased with increasing WHSV, whereas a reverse trend was found for the corresponding g value. However, we found the spin concentration increased by 69-fold, from 9.0×10^{19} at WHSV = 13 h^{-1} to 5.3×10^{21} at WHSV = 50 h^{-1}.

TABLE 1

List of EPR and NMR Parameters for Fresh and Coked H–ZSM-5 Catalysts

	Coke content (±0.1 wt%)[a]	ΔH (±0.5 G)[b]	g (±0.0001)	χ (±10%)[c]	δ_s (ppm)	λ (±0.005 nm)[d]	σ_{xe}[e]	V/V_o (%)[f]	$\Delta(V/V_o)$[g]
Fresh catalyst	—	13.1	2.0027	5.8×10^{16}	103.1 ± 0.4	0.279	3.8 ± 0.2	100	—
Coked catalyst temperature; T_c (°C)[h]									
350	3.3	9.1	2.0028	2.4×10^{18}	103.4 ± 0.4	0.277	4.7 ± 0.1	80	6.1
400	3.6	7.3	2.0028	6.5×10^{19}	104.3 ± 0.8	0.273	4.5 ± 0.1	84	4.4
450	3.4	6.9	2.0027	8.9×10^{19}	104.2 ± 1.4	0.274	4.4 ± 0.1	86	4.1
500	3.9	6.1	2.0026	9.0×10^{19}	104.8 ± 0.6	0.271	4.5 ± 0.1	84	4.1
550	4.5	3.8	2.0026	1.3×10^{20}	106.3 ± 0.4	0.264	4.6 ± 0.1	83	3.8
H_2/EB (mol/mol)[i]									
~0	3.5	5.3	2.0026	1.7×10^{20}	106.1 ± 0.3	0.265	4.4 ± 0.1	86	4.0
0.25	3.7	5.3	2.0026	2.1×10^{20}	105.5 ± 0.8	0.268	4.6 ± 0.2	83	4.6
0.50	3.9	6.1	2.0026	9.0×10^{19}	104.8 ± 0.6	0.271	4.5 ± 0.1	84	4.1
1.00	4.2	6.3	2.0026	1.3×10^{20}	103.9 ± 0.2	0.275	5.0 ± 0.1	76	5.7
WHSV (h^{-1})[j]									
13	3.9	6.1	2.0026	9.0×10^{19}	104.8 ± 0.6	0.271	4.5 ± 0.1	84	4.1
30	4.4	6.4	2.0026	1.1×10^{20}	106.1 ± 2.0	0.265	5.0 ± 0.1	76	5.5
50	3.6	6.5	2.0025	5.3×10^{21}	105.7 ± 1.8	0.267	4.9 ± 0.3	78	3.3

[a] Determined by TGA.
[b] EPR linewidth.
[c] Spin concentration, in number of spins per gram of coke.
[d] Calculated from Eq. [2], with $A = 49.9$ and $B = 0.2054$.
[e] In units of 10^{20} ppm g cat./atom.
[f] Calculated from Eq. [4].
[g] Percentage free volume per gram of coke; obtained from V/V_o divided by coke weight.
[h] Obtained at H_2/EB = 0.5; WHSV = 13 h^{-1}.
[i] Obtained at $T_c = 500$°C; WHSV = 13 h^{-1}.
[j] Obtained at $T_c = 500$°C; H_2/EB = 0.5.

^{13}C CP-MAS NMR Studies

The ^{13}C CP-MAS NMR spectra of the coked samples obtained under various reaction conditions are also depicted in Fig. 1. All spectra exhibited a broad peak in the chemical shift range 120–150 ppm. For the coked samples obtained at $T_c = 350$°C, additional peaks with relatively weaker intensities in the 20–50 ppm region were observed. The broad peak can be ascribed (25, 26) to the presence of nonsubstituted aromatic carbons (120–130 ppm), carbon bridges between aromatic rings (130–140 ppm), and substituted aromatic carbons (140–150 ppm) while the relatively weaker, well resolved signals appearing in the 20–50 ppm regions indicate the presence of aliphatic carbons. The lines of the aliphatic species may correspond to terminal methyl carbon (23 ppm) and penultimate methylene carbon (33 ppm). In other words, the results indicate that the major constituents of the coke formed at this temperature are lightweight ethyl polycyclic aromatic carbonaceous compounds. The intensities of the aliphatic resonance signals were observed to decrease with increasing T_c. For $T_c \geq 450$°C, aliphatic signals disappeared indicating the absence of lightweight, volatile soft cokes. For further increases in T_c, the aromatic peak became broader (centered at ca. 125 ppm) which indicates that only the more bulky polyaromatic cokes were retained in the sample at elevated temperatures. However, variations in the other two parameters, namely the H_2/EB ratio and WHSV, did not result in any appreciable changes in the ^{13}C NMR resonance; therefore, the nature of coke residues should remain the same.

It is known that in complex carbonaceous materials such as coal, a significant fraction of aromatic carbons are "invisible" under the ^{13}C–^{1}H cross polarization (CP) NMR experiments (27, 28). The same phenomenon has been observed in coked zeolite catalysts, especially in the samples prepared at high temperatures (29, 30). Presumably, the carbonaceous compounds (cokes) retained in the catalyst are hydrogen deficient; therefore, the dipolar coupling among the ^{13}C nuclei and the remote protons are expected to be weak. Moreover, free radicals, if present in an appreciable amount, may also interact with the surrounding ^{13}C nuclei and broaden the resonance beyond detectability. In view of the above findings, a series of ^{13}C single pulse excitation (SPE) experiments were performed especially on those samples consisting of high electron spin concentrations. In this context, the free induction decay signals were accumulated under magic-angle-spinning in the absence of proton cross-polarization where samples were subjected to

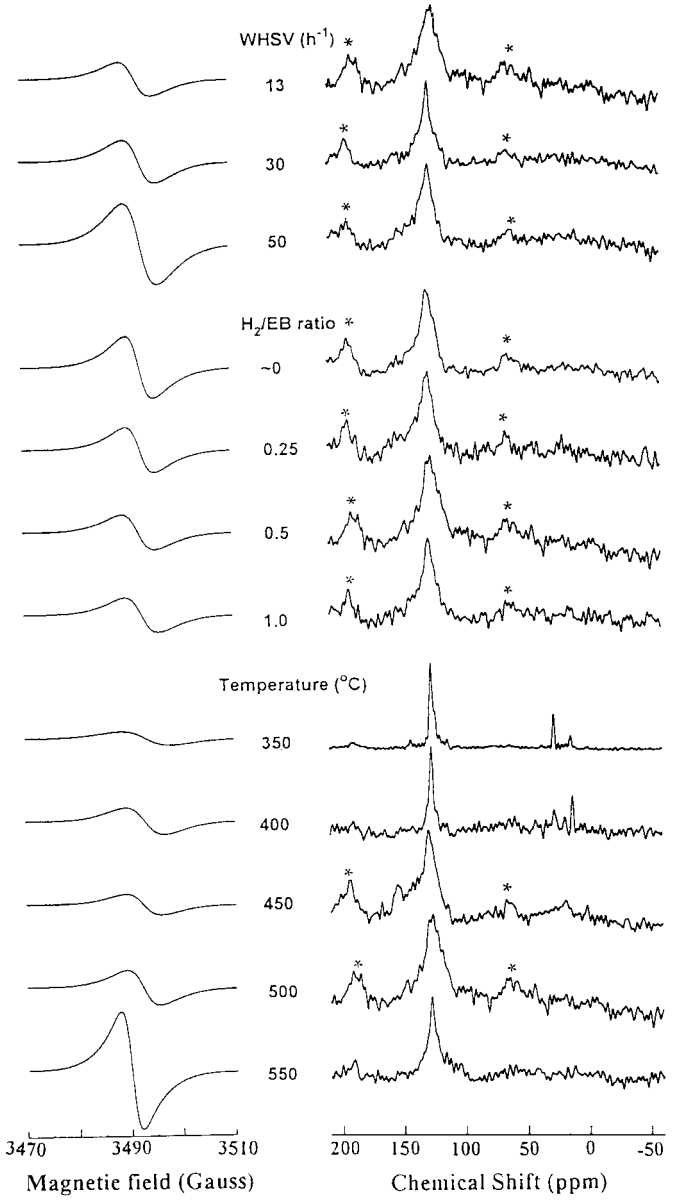

FIG. 1. EPR (left) and ^{13}C CP-MAS NMR (right) spectra of the coked H–ZSM-5 samples obtained under various reaction conditions: reaction temperatures (with constant $H_2/EB = 0.5$ and WHSV $= 13$ h^{-1}), carrier gas to feed ratios (with constant $T_c = 500°$C and WHSV $= 13$ h^{-1}), and space velocities (with constant $T_c = 500°$C and $H_2/EB = 0.5$), respectively. All ^{13}C NMR spectra were subjected to 100 Hz line broadening. The peaks denoted by an asterisk represent spinning side bands.

a single 90° pulse (pulse width 2.8 μs) with a recycle delay of 2 s. However, we observe no appreciable spectral difference between the ^{13}C MAS NMR spectra obtained by CP and SPE experiments.

Xenon Adsorption Isotherm

The isotherms of xenon adsorbed on the fresh and coked H–ZSM-5 catalysts were obtained under various reaction conditions (Fig. 2). All isotherms exhibited Langmuir-type adsorption within the pressure range covered. The adsorption capacity for xenon was observed to decrease with increasing T_c within the temperature range from 450 to 550°C. For samples prepared at $T_c < 450°$C, some volatile soft cokes may retain in the intracrystalline voids of the zeolite together with the hard cokes and hence may lower the Xe adsorption capacity even further. At first glance, the trend

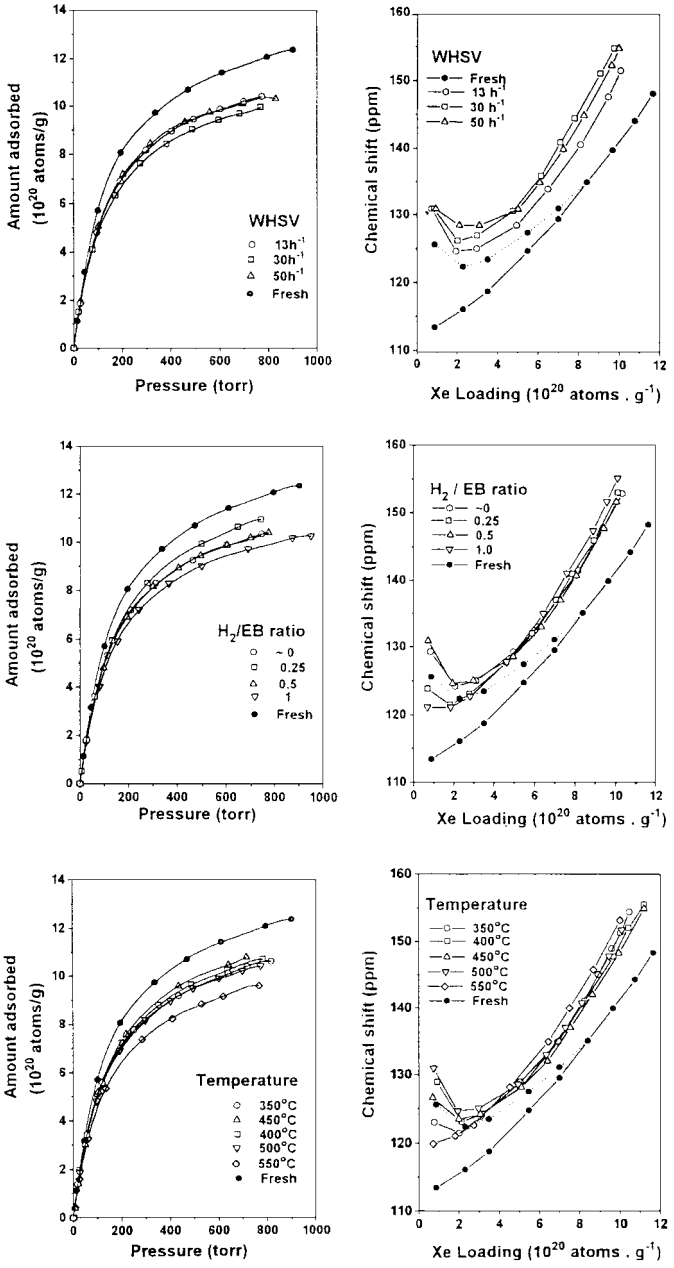

FIG. 2. Variations of room temperature xenon adsorption isotherms (left) and ^{129}Xe NMR chemical shifts with xenon loading (right) for coked H–ZSM-5 samples prepared under various reaction conditions: reaction temperatures (constant $H_2/EB = 0.5$ and WHSV $= 13$ h^{-1}), carrier gas to feed ratios (constant $T_c = 500°$C and WHSV $= 13$ h^{-1}), and space velocities (constant $T_c = 500°$C and $H_2/EB = 0.5$), respectively. The results obtained from the fresh sample were also shown for comparison.

TABLE 2

Comparisons of the Reaction Condition and Performance for Fresh and Coked H–ZSM-5 Zeolites during Ethylbenzene Disproportionation Reaction

	Fresh catalyst		Coked catalysts					
Si/Al ratio	15	33	15	15	15	15	15	33
Crystalline size (μm)	0.3	2.0	0.3	0.3	0.3	0.3	0.3	2.0
Pretreatment condition[a]								
T_c (°C)	—	—	500	550	500	500	550[b]	550[b]
H_2/EB (mol/mol)	—	—	0.5	0.5	~0	0.5	~0	~0
WHSV (h^{-1})	—	—	13	13	13	30	30	30
Performance[c]								
EB conversion (wt%)	10.4	8.3	6.0	5.5	5.6	5.4	1.4	0.3
selectivity (%)								
benzene	31.7	42.9	35.0	26.7	27.5	24.1	35.7	63.9
diethylbenzene	61.5	49.1	58.3	52.7	54.5	46.3	57.9	16.2
others	6.8	8.0	6.7	20.6	18.0	29.6	6.4	19.9
DEB isomers (%)								
p-DEB	29.7	31.6	30.1	32.6	32.4	32.3	47.0	80.7
m-DEB	65.2	68.2	69.1	66.7	66.8	66.9	50.6	19.3
o-DEB	5.1	0.2	0.8	0.7	0.8	0.8	2.4	trace

[a] Pretreatment time = 3 h.
[b] Pretreatment time = 72 h.
[c] All data were obtained under the same reaction conditions: $T_c = 265$°C, WHSV = 3.5 h^{-1}, H_2/EB = 2.0 mol/mol and TOS = 2 h, after each sample was subjected to pretreatment under respective conditions.

for the variations of Xe adsorption isotherms upon changing the space velocity and the H_2/EB ratio might not be apparent. However, a closer examination revealed that the observed Xe adsorption capacity decreases with an increasing amount of total coke (Table 1) retained in the sample.

^{129}Xe NMR Studies

The variations of ^{129}Xe NMR chemical shift as a function of xenon loading for the fresh and the coked samples prepared under various experimental conditions are shown in Fig. 2. In general, the ^{129}Xe chemical shifts were observed to decrease linearly with decreasing xenon loading. However, at very low xenon loading ($<5 \times 10^{20}$ atoms g^{-1}), an opposite trend was found showing an upward concave chemical shift curve. In general, such phenomena are more pronounced for the coked samples that have higher electron spin concentrations (Table 1). A similar phenomenon was also observed by Ryoo *et al.* (31) in their study of solid state defects in H–ZSM-5 zeolites. The authors attributed such a phenomenon to the formation of free radicals and solid state defects during high temperature evacuation of the zeolite samples.

In general, the observed ^{129}Xe chemical shifts at high xenon loading in Fig. 2 can be described by the linear equation (32, 33)

$$\delta(\rho) = \delta_o + \delta_s + \sigma_{xe}\rho, \qquad [1]$$

where $\delta_o = 0$ is the chemical shift reference and ρ represents the xenon density. The term δ_s is the chemical shift at zero xenon loading ($\rho = 0$) and can be divided into the sum of two contributions: the part arising from the interactions between Xe and the zeolite walls and that between Xe and the coke residues. The value of δ_s can readily be obtained by extrapolating the straight line to the chemical shift axis. The last term is characteristic of the Xe–Xe interactions and is proportional to the density of the adsorbed Xe. The value of σ_{xe} which may be obtained from the slope of the $\delta(\rho)$ vs ρ plot represents the first-order coefficient in the virial expansion of the total chemical shift. The related parameters obtained from ^{129}Xe NMR studies are listed in Table 2. For obvious reasons, only those data corresponding to xenon loading greater than 5×10^{20} atoms g^{-1} were considered in estimating the NMR parameters. The variations in the NMR parameters (Table 2) indicate that the nature and the location of coke residues vary significantly with the experimental conditions.

DISCUSSION

The Nature and Formation of Coke

It was reported that coking in zeolites leads to the formation of free radicals, which may be characterized by EPR spectroscopy. Although the typical concentration of the free radicals is only about one per 1000–10,000 carbon atoms, it has been demonstrated (23, 24, 34) that valuable information such as the nature and composition of cokes may be deduced from the EPR measurements. Even for a system that yields EPR spectra with no hyperfine splitting, some

useful information can still be deduced from the g value, spin concentration, and linewidth of the EPR signal.

We found that the EPR parameters of the coked samples depended greatly on reaction temperature. The spectral narrowing observed at higher T_c may arise from (i) spin–spin interaction, as the spin concentration increases at high T_c, and (ii) extensive spin delocalization among multiple aromatic rings of the coke residues. This is supported by the decrease in the g value at higher T_c where the g values obtained from the samples coked at high T_c seemingly approach the free electron value ($g = 2.0023$) as the electron spin becomes more delocalized. The increase in the spin concentration and the decrease in the EPR linewidth are more pronounced when $T_c \geq 400^\circ$C. For $T_c = 350^\circ$C, the presence of aliphatic and less bulky aromatic soft cokes give rise to a broadening of the EPR resonance with greater g values. We may conclude from the EPR studies that an increase in the reaction temperature yields an increase in aromaticity of carbonaceous compounds through the formation of condensed polycyclic aromatic compounds. We also noticed that the change in the nature of the coke is more pronounced at $T_c \geq 400^\circ$C as judged from the changes in linewidth and spin concentration.

^{13}C CP-MAS NMR spectroscopy provides a nondestructive technique for direct characterization of cokes deposited in porous catalysts such as zeolites. Earlier studies have demonstrated (21, 22, 35, 36) that the nature and the state of the carbonaceous residues retained in zeolites can be inferred from the chemical shift, linewidth, and relaxation times data. In general, mobile species normally exhibit narrow, well-resolved ^{13}C resonance lines while more condensed carbonaceous compounds normally yield a broad, featureless line. For the former, a major contribution may arise from volatile and/or physically adsorbed (soft) cokes, coke precursors, and retained reactants or products. In most cases, these mobile species can be removed by simple sample evacuation treatment (21, 22). For the latter, the broad resonance is normally ascribed to the bulky, polyaromatic (hard) coke which cannot be removed easily unless the fouled catalyst is subjected to regeneration (e.g., through combustion) treatment at elevated temperatures. Accordingly, the ^{13}C CP-MAS NMR spectra shown in Fig. 2 clearly indicate that, at low reaction temperatures ($<400^\circ$C), cokes consist of lightweight, mobile alkyl aromatic compounds, whereas, at higher reaction temperatures, the cokes are more condensed and are polycyclic aromatic in nature. This is consistent with the EPR results presented above.

The presence of H_2 carrier gas is known to reduce the deactivation rate of the zeolite catalysts during hydrocarbon transformations. The dissociate adsorption of H_2 over many active sites was found (37) to be responsible for the persistence of catalyst activity. Accordingly, upon varying the H_2/EB ratio, no notable change in the g value was observed (Table 1) while only a marginal decrease in the spin concentrations and a slight increase in the EPR linewidths were found. We may therefore conclude that variation in the H_2/EB ratio have a marginal effect on the nature and composition of coke residues. This is further confirmed by the ^{13}C NMR results (Fig. 1) where no appreciable change in the spectral features was observed.

On the effect of space velocity variation, while only a slight increase in spin concentration was observed when the space velocity was increased from 13 to 30 h^{-1}, a sudden increase of spin concentration at WHSV = 50 h^{-1} was observed. No noticeable changes in spectral parameters such as linewidth and g value with a change in WHSV were observed. Nor did we find much effect on the spectral features of the ^{13}C NMR signals (Fig. 1). Thus, similar to that observed during H_2/EB variations, changes in space velocity have no appreciable effect on the nature of cokes except maybe at very high WHSV of 50 h^{-1}. In summary, our EPR and ^{13}C NMR studies yield consistent results indicating that the nature and composition of cokes formed during EB disproportionation over H-ZSM-5 zeolite strongly depend on the reaction temperature. A much weaker dependence was found for the variations in carrier gas concentration and in space velocity, except when the reaction is carried out at very high WHSV $\geq$ 50 h^{-1}.

Coke Induced Selectivation

As described earlier, the intercept of the $\delta(\rho)$ vs ρ plot (Fig. 2), $\delta_s(\rho = 0)$, can be ascribed to the chemical shift contribution arising from the interactions between xenon atoms and the intracrystalline walls of the zeolite. Hence, in principle, the value of δ_s can be correlated to the structural parameters (such as channel diameter) of zeolites. Fraissard *et al.* (32, 38, 39) had proposed an empirical relation between δ_s and the average xenon mean-free-path (denoted by λ; in unit of nm) for a variety of different zeolites as

$$\delta_s = A/(B + \lambda), \qquad [2]$$

where $A = 49.9$ and $B = 0.2054$. For zeolites with ideal (infinitely long, straight, and cylindrical) intracrystalline channels, λ can be related to the channel diameter of the zeolite (D_{zeolite}) by

$$\lambda = D_{\text{zeolite}} - D_{\text{xe}}, \qquad [3]$$

where $D_{\text{xe}} = 0.44$ nm is the kinetic diameter of the xenon atom. Taking the observed value of $\delta_s = 103.1$ ppm (Table 2), the estimated effective channel diameter of the fresh ZSM-5 zeolite is 0.719 nm. Although the calculated value is in good agreement with that previously reported by Tsiao *et al.* (Ref. (40); 0.72 nm), it is too big to account for either type of the channels which exist in ZSM-5 zeolites. Two types of channels are known to exist in ZSM-5 zeolites, the straight, near-circular (0.53 nm $\times$ 0.56 nm) channels are

parallel to the [010] plane cross-linked by the zigzag, and the other elliptical (0.51 nm × 0.55 nm) channels which are parallel to the [100] plane (41).

To evaluate the variation of average xenon mean-free-path in the presence of intracrystalline coke residues, the λ values for each coked sample were calculated by using Eq. [2] and are summarized in Table 1. We found that regardless of the amount of cokes present in each sample, the values of λ for the coked samples differ only marginally from that of the fresh catalyst ($\lambda = 0.279$ nm; see Table 1). Nevertheless, the trend in the variations of λ indicate that the diffusion constraints imposed on the adsorbed Xe, as reflected by the diminishing λ, increase with increasing reaction temperature or decreasing H_2/EB ratio. However, no specific trend in the variation of λ with space velocity was found. It will be shown later that the increase in the diffusion constraints for the adsorbed Xe molecules is due to the preferential deposition of cokes near the channel opening and on the external surfaces of the zeolite crystallites.

An alternative approach to the problem is through the analysis of the slopes (σ_{xe}) of the chemical shift at high xenon loading. It is generally accepted that the value of σ_{xe} is inversely proportional to the effective pore volume of the zeolite (20, 38, 42–44). The relative internal free volume accessible to xenon gas per gram of catalyst can be expressed as

$$V/V_o = (\sigma_{xe})_{fresh}/(\sigma_{xe})_{coked}, \quad [4]$$

where V and V_o are the internal volumes of the coked and the fresh samples, respectively. The calculated values of V/V_o are listed in Table 1. Overall, the presence of cokes on H–ZSM-5 resulted in a decrease of internal free volume in comparison to the fresh catalyst. It should be noted that the NMR parameters so derived possess only limited accuracy compared to that estimated by a conventional structural analysis technique such as X-ray diffraction. Nevertheless, ^{129}Xe NMR spectroscopy has been shown to be a unique and practical technique not only for structural characterization of zeolites (38, 45–47), but also for examining the variation of zeolite pore dimensions during adsorption (48), coking (19–21, 40, 43), and ion-exchange (49) that otherwise is extremely difficult, if not impossible, by conventional techniques. In this context, the qualitative interpretations of the NMR parameters obtained from the fresh and coked samples are provided rather than the quantitative comparison.

Upon varying the reaction temperature from 350 to 450°C, we found a notable increase in the internal free volume even though the samples have a comparable coke content (Table 1). Further increase in T_c from 450 to 550°C, on the other hand, resulted in a marked increase in coke content with a slow decrease in V/V_o. However, a clear trend was found when the relative changes in effective free volume were calculated in terms of per gram coke formed in the samples, as denoted by $\Delta(V/V_o)$ in Table 1. Accordingly, when T_c was increased from 350 to 550°C, a steady decrease in the fractional change in the effective free volume per gram of coke from 6.1 to 3.8 was observed.

It is noted that, at $T_c = 350$°C, the notable decrease in effective free volume is mainly due to the retention of the soft cokes within the intracrystalline channels of the H–ZSM-5 zeolite. This notion is supported by both the ^{13}C NMR and the EPR results (*vide supra*). For $T_c \geq 400$°C, while the coke content increases with increasing T_c, an opposite trend found for $\Delta(V/V_o)$ can only be explained by the preferential deposition of cokes on the external surface of zeolite crystallites. Moreover, as indicated in the ^{13}C NMR and EPR spectra, the aromaticity of coke was increased with increasing temperature. Thus, those external carbonaceous residues should be bulky hard cokes with polyaromatic compounds in nature. Previously, some preferential deposition of external coke at high reaction temperature and vice versa for internal coke during toluene disproportionation over H–ZSM-5 zeolite was also reported by Rozwadowski *et al.* (16).

At constant $T_c = 500$°C and with WHSV = 13 h^{-1}, the variation of H_2/EB ratio from ~0 to 1.0 resulted in a gradual decrease in V/V_o. This is in accordance with the corresponding increase in the amount of total cokes from 3.5 to 4.2 wt%. However, an overall increase in the corresponding $\Delta(V/V_o)$ values was found to increase with H_2/EB ratio. In other words, at low H_2 carrier gas concentration, cokes seemingly prefer to deposit on the external surface of the zeolite crystallites. It is noted that soft cokes are unlikely to form at such high temperature (500°C). This is in agreement with the observed ^{13}C NMR results (Fig. 1) and the EPR parameters (Table 1). Moreover, the H_2 as a carrier gas is known to serve not only as a diluent medium, but also as an active participant in the hydrocarbon conversion. Guisnet and co-workers (50, 51) reported that, during toluene disproportionation over mordenite, the presence of H_2 carrier gas could affect the equilibrium formation of the carbonium ions (reaction intermediates) and hence resulted in a decrease in the reaction rate. More recently, Chen *et al.* (22) further revealed that, during cumene disproportionation over zeolite beta, H_2 molecules might hydrogenate with reaction intermediates and/or cokes to form partially hydrogenated polycyclic aromatic carbonaceous compounds. Thus, we propose that, at higher H_2/EB ratio, the carbonaceous deposits are less bulky in nature and tend to locate within the intracrystalline voids of zeolite whereas at low H_2/EB ratios, more bulky cokes are formed on the outer surface of the crystallites. However, the structural differences of these carbonaceous compounds may be too small to be noted by the ^{13}C NMR or EPR spectroscopic techniques.

Upon varying the space velocity while keeping $T_c =$ 500°C and H_2/EB = 0.5 mol/mol, no apparent trend for the

coke content and internal free volume can be found. However, a marginal decrease in λ with increasing WHSV is noticed suggesting an increase in diffusion constraints to the adsorbed Xe. The diffusion constraints imposed on the reactants, products, and reaction intermediates should, in turn, favor the product shape selectivity.

To examine the effect of coking on product selectivity and to attain a common basis for easy comparison, all samples were brought to the moderate reaction conditions ($T_c = 265^\circ$C, H_2/EB = 2.0 mol/mol, WHSV = 3.5 h^{-1}) after the primary coking pretreatment. The corresponding pretreatment conditions and the performance of the coked catalysts are listed in Table 2 together with the product distribution over the fresh catalyst. In the ethylbenzene disproportionation reaction, we determine the *para*-selectivity of diethylbenzene (DEB) as the amount of *p*-DEB divided by the total amount of DEB isomers, which should reflect the coke-induced shape selectivity of the H–ZSM-5 zeolite. In the fresh catalyst without pretreatment, this ratio was found to be 29.7%. The ratio increased slightly to 30.1% when the sample was subjected to the following coking pretreatment conditions: $T_c = 500^\circ$C, H_2/EB = 0.5 mol/mol, and WHSV = 13 h^{-1}. By changing T_c (to 550°C), H_2/EB ($\sim$0 mol/mol), and WHSV (to 30 h^{-1}), the *p*-DEB selectivity increased to 32.6, 32.4, and 32.3%, respectively. Moreover, under optimized conditions ($T_c = 550^\circ$C, H_2/EB $\sim$ 0 mol/mol, and WHSV = 30 h^{-1}) in a prolonged coking (72 h) run, the *p*-DEB selectivity increased to 47.0 %. However, the ethylbenzene conversion decreased to 1.4 wt% in the process. We must point out that such a variation in shape selectivity is significant in view of the small crystalline size (ca. 0.3 μm) of the H–ZSM-5 zeolite used in our study. Furthermore, when a complementary experiment over large ZSM-5 crystalline (ca. 2 μm) sample was used for the coking study, a more significant increase in *p*-DEB selectivity (to 80.7%) was observed. Note that the *p*-DEB selectivity is only 31.6% for the fresh large crystallite sample (Table 2). Such a coke-induced selectivation is ascribed to the preferred deposition of the external cokes which modify the surface acid properties of the zeolite, thus effectively hindering the secondary isomerization pathways of *p*-DEB, and to some extent increasing the diffusion constraints for the reactant and product molecules. Further experiments are in progress in this laboratory to realize more significant shape selectivity.

CONCLUSIONS

We have demonstrated that the selective deposition of coke can be used as a modifying agent for the selectivation of H–ZSM-5 zeolite during ethylbenzene disproportionation. It is found that increasing the reaction temperature results in an increase in the aromaticity of coke residues, while changing the space velocity and H_2/EB molar ratio do not result in notable changes in the structural nature and composition of the coke. Finally, an increase in reaction temperature, a decrease in H_2/EB molar ratio, or an increase in the space velocity of the ethylbenzene favor the formation of external coke. The deposition of external coke effectively modifies the surface acid properties of the zeolite crystallites which, in turn, inhibits the secondary isomerization pathways of *p*-diethylbenzene and/or induces diffusion constraints, and thus enhances the *para*-selectivity.

ACKNOWLEDGMENTS

The financial supports of this work by the National Science Council, Republic of China (NSC87-2113-M001-003 and NSC88-2113-M001-008) are gratefully acknowledged. We thank the reviewers for many useful comments.

REFERENCES

1. Chen, N. Y., Garwood, W. E., and Dwyer, F. G., "Shape Selective Catalysis in Industrial Applications," *Chem. Ind. Ser.*, Vol. 36. Dekker, New York, 1989.
2. Chen, N. Y., Degnan, T. F., Jr., and Morris Smith, C., "Molecular Transport and Reactions in Zeolites: Design and Application of Shape Selective Catalysts," p. 206. VCH, New York, 1994.
3. Kim, J. H., Kunieda, T., and Niwa, M., *J. Catal.* **173**, 433 (1998).
4. Shiralkar, V. P., Joshi, P. N., Eapen, M. J., and Rao, B. S., *Zeolites* **11**, 511 (1991).
5. Chen, N. Y., Keading, W. W., and Dwyer, F. G., *J. Am. Chem. Soc.* **101**, 6783 (1979).
6. Niwa, M., Kato, M., Hattori, T., and Murakami, Y., *J. Phys. Chem.* **90**, 6233 (1986).
7. Handreck, G. P., and Smith, T. D., *Zeolites* **10**, 746 (1990).
8. Bhat, Y. S., and Halgeri, A. B., *Appl. Catal. A* **101**, 95 (1993).
9. Wang, I., Lee, B. J., and Chen, M. H., U.S. Patent 4,849,386 (1989).
10. Wang, I., Lee, B. J., and Chen, M. H., *Appl. Catal. A* **54**, 257 (1989).
11. Uguina, M. A., Sotelo, J. L., Serrano, D. P., Van Grieken, R., and Venes, S., *Ind. Eng. Chem. Res.* **31**, 1875 (1992).
12. Kim, J. H., Ishida, A., Okajima, M., and Niwa, M., *J. Catal.* **161**, 387 (1996).
13. Haag, W. O., and Olson, D. H., U.S. Patent 4,097,543 (1978).
14. Uguina, M. A., Serrano, D. P., Van Grieken, R., and Venes, S., *Appl. Catal. A* **99**, 97 (1993).
15. Èejka, J., Pilková, N., Wichterlová, B., Eder-Mirth, G., and Lercher, J. A., *Zeolites* **17**, 265 (1996).
16. Rozwadowski, M., Wloch, J., Erdmann, K., and Kornatowski, J., *Coll. Czech. Chem. Commun.* **57**, 959 (1992).
17. Bhat, Y. S., Das, J., and Halgeri, A. B., *J. Catal.* **155**, 154 (1995).
18. Melson, S., and Schüth, F., *J. Catal.* **170**, 46 (1997).
19. Fang, L. Y., Liu, S. B., and Wang, I., *J. Catal.*, in press.
20. Pradhan, A. R., Wu, J. B., Jong, S. J., Chen, W. H., Tsai, T. C., and Liu, S. B., *Appl. Catal. A* **159**, 187 (1997).
21. Liu, S. B., Prasad, S., Wu, J. F., Ma, L. J., Yang, T. C., Chiou, J. T., Chang, J. Y., and Tsai, T. C., *J. Catal.* **142**, 664 (1993).
22. Chen, W. H., Pradhan, A. R., Jong, S. J., Lee, T. Y., Wang, I., Tsai, T. C., and Liu, S. B., *J. Catal.* **163**, 436 (1996).
23. Lange, J. P., Gutsze, A., and Karge, H. G., *J. Catal.* **114**, 136 (1988).
24. Karge, H. G., Lange, J. P., Gutsze, A., and Laniecki, M., *J. Catal.* **114**, 144 (1988).
25. Stothers, J. B., "Carbon-13 NMR Spectroscopy," p. 90. Academic Press, New York, 1972.
26. Silverstein, R. M., Basslers, G. C., and Morvill, T. C., "Spectroscopic Investigation of Organic Compounds," Chap. 5. Wiley, New York, 1991.

27. Sullivan, M. J., and Macel, G. E., *Anal. Chem*. **54**, 1615 (1982).
28. Dudley, R. L., and Fyfe, C. A., *Fuel* **61**, 651 (1982).
29. Richardson, B. R., and Haw, J. F., *Anal. Chem*. **61**, 1821 (1989).
30. Snape, C. E., McGhee, B. J., Anderson, J. M., Hughes, R., Koon, C. L., and Hutching, G., *Appl. Catal. A* **129**, 125 (1995).
31. Ryoo, R., Ihee, H., Kwak, J. H., Seo, G., and Liu, S. B., *Micro. Mater.* **4**, 59 (1995).
32. Demarquay, J., and Fraissard, J., *Chem. Phys. Lett.* **136**, 314 (1987).
33. Cheung, T. T. P., and Fu, C. M., *J. Phys. Chem*. **93**, 3740 (1989).
34. Karge, H. G., and Boldingh, E. P., *Catal. Today* **3**, 53 (1988).
35. Bonardet, J. L., Barrage, M. C., and Fraissard, J., *J. Mol. Catal. A* **96**, 123 (1995).
36. Ivanova, I. I., and Derouane, E. G., *Stud. Surf. Sci. Catal.* **85**, 357 (1994).
37. Bauer, F., Ernst, H., Geidel, E., and Schodel, R., *J. Catal.* **164**, 146 (1996).
38. Fraissard, J., and Ito, T., *Zeolites* **8**, 350 (1988).
39. Benslama, R., Fraissard, J., Albizane, A., Fajula, F., and Figueras, F., *Zeolites* **8**, 196 (1988).
40. Tsiao, C., Dybowski, C., Gaffney, A. M., and Sofranko, J. A., *J. Catal.* **128**, 520 (1991).
41. Kokotailo, G. T., Lawton, S. L., Olson, D. H., and Meier, W. M., *Nature* **272**, 437 (1978).
42. Cheung, T. T. P., *J. Phys. Chem*. **93**, 7549 (1989).
43. Chen, W. H., Jong, S. J., Pradhan, A., Lee, T. Y., Wang, I., Tsai, T. C., and Liu, S. B., *J. Chin. Chem. Soc.* **43**, 305 (1996).
44. Johnson, D. W., and Griffiths, L., *Zeolites* **7**, 484 (1987).
45. Dybowski, C., Bansal, N., and Duncan, T. M., *Ann. Rev. Phys. Chem*. **42**, 433 (1991).
46. Barrie, P. J., and Klinowski, J., *Prog. NMR Spectro.* **24**, 91 (1992).
47. Raftery, D., and Chmelka, B. F., "NMR Basic Principle and Progress," Vol. 30, p. 110. Springer-Verlag, Berlin, 1994.
48. Liu, S. B., Ma, L. J., Lin, M. W., Wu, J. F., and Chen, T. L., *J. Phys. Chem*. **96**, 8120 (1992).
49. Liu, S. B., Fung, B. M., Yang, T. C., Hong, E. C., and Chang, C. T., *J. Phys. Chem*. **98**, 4393 (1994).
50. Gnep, N. S., and Guisnet, M., *Appl. Catal.* **1**, 329 (1981).
51. Guisnet, M., *J. Catal.* **88**, 249 (1984).